



Article

Deriving Verified Vehicle Trajectories from LiDAR Sensor Data to Evaluate Traffic Signal Performance

Enrique D. Saldivar-Carranza *  and Darcy M. Bullock 

Joint Transportation Research Program, Lyles School of Civil Engineering, Purdue University, West Lafayette, IN 47907, USA; darcy@purdue.edu

* Correspondence: esaldiva@purdue.edu

Abstract: Advances and cost reductions in Light Detection and Ranging (LiDAR) sensor technology have allowed for their implementation in detecting vehicles, cyclists, and pedestrians at signalized intersections. Most LiDAR use cases have focused on safety analyses using its high-fidelity tracking capabilities. This study presents a methodology to transform LiDAR data into localized, verified, and linear-referenced trajectories to derive Purdue Probe Diagrams (PPDs). The following four performance measures are then derived from the PPDs: arrivals on green (AOG), split failures (SF), downstream blockage (DSB), and control delay level of service (LOS). Noise is filtered for each detected vehicle by iteratively projecting each sample's future location and keeping the subsequent sample that is close enough to the estimated destination. Then, a far side is defined for the analyzed intersection's movement to linear reference sampled trajectories and to remove those that do not cross through that point. The technique is demonstrated by using over one hour of LiDAR data at an intersection in Utah to derive PPDs. Signal performance is then estimated from these PPDs. The results are compared to those obtained from comparable PPDs derived from connected vehicle (CV) trajectory data. The generated PPDs from both data sources are similar, with relatively modest differences of 1% AOG and a 1.39 s/veh control delay. Practitioners can use the presented methodology to estimate trajectory-based traffic signal performance measures from their deployed LiDAR sensors. The paper concludes by recommending that unfiltered LiDAR data are used for deriving PPDs and extending the detection zones to cover the largest observed queues to improve performance estimation reliability.



Citation: Saldivar-Carranza, E.D.; Bullock, D.M. Deriving Verified Vehicle Trajectories from LiDAR Sensor Data to Evaluate Traffic Signal Performance. *Future Transp.* **2024**, *4*, 765–779. <https://doi.org/10.3390/futuretransp4030036>

Received: 26 April 2024

Revised: 13 June 2024

Accepted: 4 July 2024

Published: 9 July 2024

Keywords: LiDAR; trajectory; traffic signal; performance measures; connected vehicle

1. Introduction

Light Detection and Ranging (LiDAR) technology estimates the relative location of surrounding objects and surfaces by calculating the round-trip delay of light signals generated by lasers. In a LiDAR system, a transmitter emits light, and a receiver gathers the bounced signal and computes its traveled distance. A collection of distance measurements in a specific environment creates a point cloud, which is a three-dimensional representation of the space [1]. From the point cloud, diverse characteristics of the environment can be analyzed, and objects can be identified and tracked.

The use of LiDAR sensors has increased across state transportation agencies. The main reasons for this growth are an increase in the knowledge and acceptance of the technology and its cost-effectiveness benefits in comparison with other conventional surveying techniques [2,3].

Emerging uses of LiDAR in transportation include bridge assessment [4], road mapping [5], pavement analysis [6,7], and traffic sign inventories [8,9]. In the area of mobility, safety assessments have been the focus of LiDAR applications due its mode detection and tracking capabilities [10,11]. Bandaru et al. created a device and designed algorithms to identify traffic conflicts, analyze speeds, and visualize the presence of pedestrians at road



Copyright: © 2024 by the authors. Licensee MDPI, Basel, Switzerland. This article is an open access article distributed under the terms and conditions of the Creative Commons Attribution (CC BY) license (<https://creativecommons.org/licenses/by/4.0/>).

intersections or segments [12]. Ansariyar deployed two LiDAR sensors at an intersection to identify crash-prone areas by evaluating near-misses [13]. Kilani et al. used this technology to evaluate sight distance challenges at urban intersections [14].

In addition to evaluating intersection safety, LiDAR data can also be utilized to generate traffic signal performance measures. Traffic signal operations have a significant impact on road transportation networks [15,16]. It is therefore important for agencies to actively monitor performance at this type of intersection to identify locations where signal retiming [17,18] or capital investment [19] can improve operations.

LiDAR data are able to replicate not only detector-based [20] but also more reliable [21,22] trajectory-based traffic signal performance measures [23–26], such as

- Arrivals on green (AOG): this operational measurement indicates the level of progression at an intersection by providing the percentage of vehicles that traverse without stopping.
- Split failures (SF): this operational measurement indicates the level of congestion at an intersection by providing the percentage of vehicles that stop more than once during their approach; that is, the percentage of vehicles that wait longer than one cycle length before crossing.
- Downstream blockage (DSB): this operational measurement indicates the level of obstruction that an adjacent intersection induces at the studied location. DSB is calculated as the percentage of vehicles that experience significant delay after crossing.
- Control delay: this delay measurement quantifies the effects that a traffic control device, such as a traffic signal, has on travel time. Traditionally, control delay has been used to assign a Highway Capacity Manual (HCM) level of service (LOS) rating (Table 1) to analyzed intersections [27].

Table 1. LOS criteria for signalized intersections.

LOS	Weighted Avg. Control Delay (s/veh)	Description
A	≤ 10	Exceptionally favorable progression
B	>10–20	Highly favorable progression
C	>20–35	Favorable progression
D	>35–55	Ineffective progression
E	>55–80	Unfavorable progression
F	>80	Very poor progression

1.1. Motivation

Recently, trajectory-based traffic signal performance measures have been derived from commercial connected vehicle (CV) trajectory data [23]. The CV dataset provides significant scalability benefits as it has nationwide coverage, but has representativeness challenges as it only counts with a small sample of all traversing vehicles [23,28]. Nevertheless, this is not a limitation of LiDAR-derived trajectory data, as they represent almost all vehicles entering the intersection. For this reason, the performance measures derived from LiDAR systems can be much more robust than those obtained from CV data and transportation agencies can immediately act upon the results.

Traffic delay were previously calculated from LiDAR sensors at signalized intersections [29]. However, no prior research has been identified on the use of LiDAR's vehicle trajectory detection capabilities to derive trajectory-based traffic signal performance measures such as AOG, SF, and DSB.

1.2. Objective and Paper Structure

The objective of this study is to provide an accurate technique to estimate movement-level traffic signal AOG, SF, DSB, control delay, and LOS from LiDAR-derived data. The following paper structure is as follows:

- Section 2. provides a summary of the datasets used in the study.

- Section 3.1. describes the study location.
- Section 3.2. presents the technique used to prepare LiDAR data to evaluate the movement-level traffic signal performance.
- Section 3.3. explains how to linear reference the selected data in order to create a Purdue Probe Diagram (PPD), which is a time–space visualization of the trajectories from which the desired performance measures can be calculated.
- Section 4. provides a comparison of the performance estimations derived from LiDAR and CV PPDs.
- Section 5. presents a discussion of the study.

2. Datasets

The two-dimensional LiDAR data of tracked objects collected on 30 December 2022, from 15:49:25 to 17:14:00 h. and CV trajectory data collected on August 2021 weekdays from 15:49:25 to 17:14:00 h. were used in this study. This section describes each dataset.

2.1. LiDAR Trajectories

This dataset contains two-dimensional trajectories of traversing objects at a signalized intersection in Utah and is published in an open access repository [30]. The dataset was derived from three-dimensional point cloud data [1] of the environment generated from four solid-state LiDAR sensors installed at each corner of the intersection.

The dataset consists of the set of estimated waypoints of traversing objects with a tenth-of-a-second sampling frequency. Each waypoint includes the following information: timestamp, x-location, y-location, speed, heading, length, number of points reflected, and an anonymous object identifier. It is important to note that this dataset does not include the information of any object traveling below 10 mph.

By linking individual waypoints with the same object identifier and sorting them by timestamp, a complete chronological object journey can be obtained. Therefore, a LiDAR-derived trajectory T_L of a particular object is defined as the set of its waypoints W_{Li} , with $i = 1, 2, \dots, k$, where $i = 1$ is the first collected sample of the object and $i = k$ is the last sample collected of the same object.

$$T_L = \{W_{Li}\}_{i=1}^k \quad (1)$$

$$W_{Li} = \{\text{identifier}, x - \text{location}_i, y - \text{location}_i, \text{timestamp}_i, \text{speed}_i, \text{heading}_i, \text{length}_i, \text{points}_i\} \quad (2)$$

Limitations

The main challenge in using LiDAR-derived trajectory data is that the detection area is limited. If increased visibility is desired, additional sensors need to be installed, which can increase costs and maintenance requirements. Additionally, adverse weather conditions can also affect measurements [31].

2.2. Connected Vehicle Trajectories

Commercially available CV trajectory data have a typical market penetration rate (MPR) of 3–7% [28]. In this study, CV trajectory data were obtained from a third-party provider with an estimated MPR of approximately 3% at the evaluated location.

The dataset consists of a set of waypoints for entire vehicle trips (i.e., from on to off). The data were collected from passenger vehicles that were factory-equipped with the required technology for sampling and transmission. There is typically a three-second reporting interval between samples, each with a three-meter (~10 ft.) spatial accuracy. Every waypoint has the following information: latitude, longitude, speed, heading, and an anonymous vehicle trajectory identifier.

By linking individual waypoints with the same vehicle trajectory identifier and sorting them by timestamp, a complete chronological vehicle journey can be obtained. Therefore, a CV-derived trajectory T_{CV} for the same vehicle is defined as the set of its waypoints W_{CVi} ,

with $i = 1, 2, \dots, k$, where $i = 1$ is the first sample collected after the vehicle is turned on and $i = k$ is the last sample collected before the vehicle is turned off.

$$T_{CV} = \{W_{CVi}\}_{i=1}^k \quad (3)$$

$$W_{CVi} = \{\text{identifier}, \text{longitude}_i, \text{latitude}_i, \text{timestamp}_i, \text{speed}_i, \text{heading}_i\} \quad (4)$$

A detailed description of the acquisition, storage, data access, and costs of the CV dataset is available in [23].

Limitations

The CV trajectory data used for this study have a latency from 30 to 60 s, which is not fast enough to be used in the real-time analysis and control of signalized intersections. Additionally, the currently available low MPR requires the aggregation of data over several days to obtain representative performance measures. Using this approach, operational irregularities on a cycle-by-cycle basis are difficult to detect. For this reason, cycle-by-cycle performance evaluations using CV data are not yet feasible [23].

Another limitation of the CV dataset is that it only contains information about passenger vehicles. Additional datasets would have to be evaluated if other vehicle classes or modes of transportation need to be evaluated.

3. Methodology

This section first provides a brief description of the studied location. Then, the proposed technique to extract valid vehicle trajectories from the LiDAR-derived data is presented. Finally, the process used to linearly reference the validated vehicle trajectories in a PPD [23] to estimate signal performance measures is provided.

3.1. Study Location

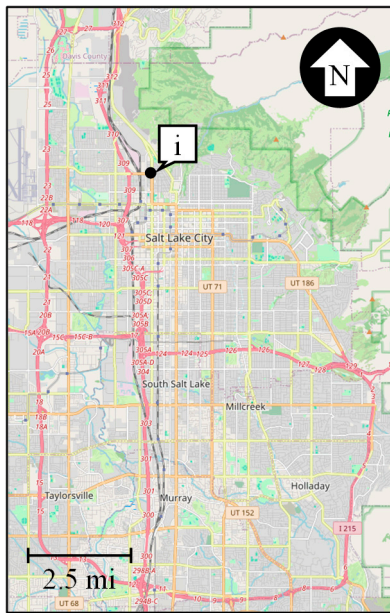
In this study, traffic signal performance was estimated for the northbound (NB) through movement at the US-89 and 600 N intersection located in a suburban area of Salt Lake City, Utah (Figure 1). This signalized intersection is managed by the Utah Department of Transportation (UDOT) and usually serves Annual Average Daily Traffic (AADT) values of under 25,000 vehicles per day on each of its approaches [32].

The LiDAR sensors installed at this location were implemented for testing purposes. The LiDAR sensor at the northeast corner (Figure 1b, callout ii) serves as the origin of the estimated object locations [30].

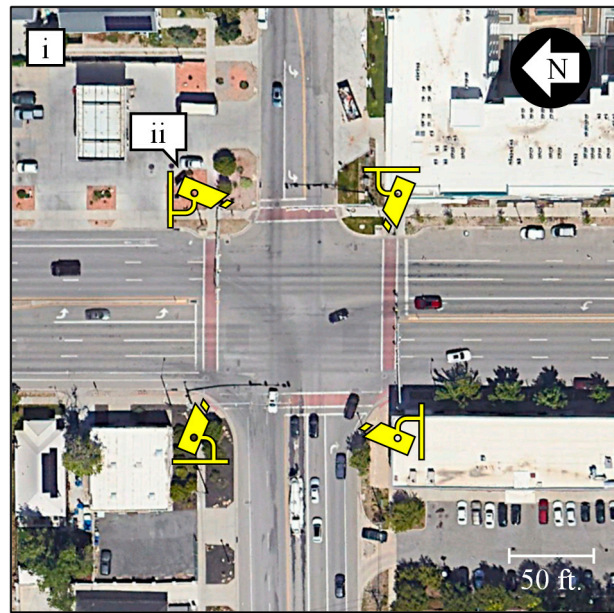
3.2. Relevant Vehicle Trajectory Extraction

Figure 2 depicts all the sampled moving objects detected by the LiDAR sensors in Figure 1b during the analysis period. These data cannot be utilized in their raw state for estimating movement-level traffic signal performance measures. The following process was used to prepare and filter the data for the subsequent derivation of movement-level traffic signal performance measures:

1. Identify noise in the data.
2. Verify likely accurate trajectories and filter unreliable samples.
3. Select pertinent vehicle trajectories for the movement of interest based on the intersection geometric features.



(a) Salt Lake City, Utah (map data: OpenStreetMap contributors)



(b) US-89 at 600 N (map data: Google)

Figure 1. Study location.

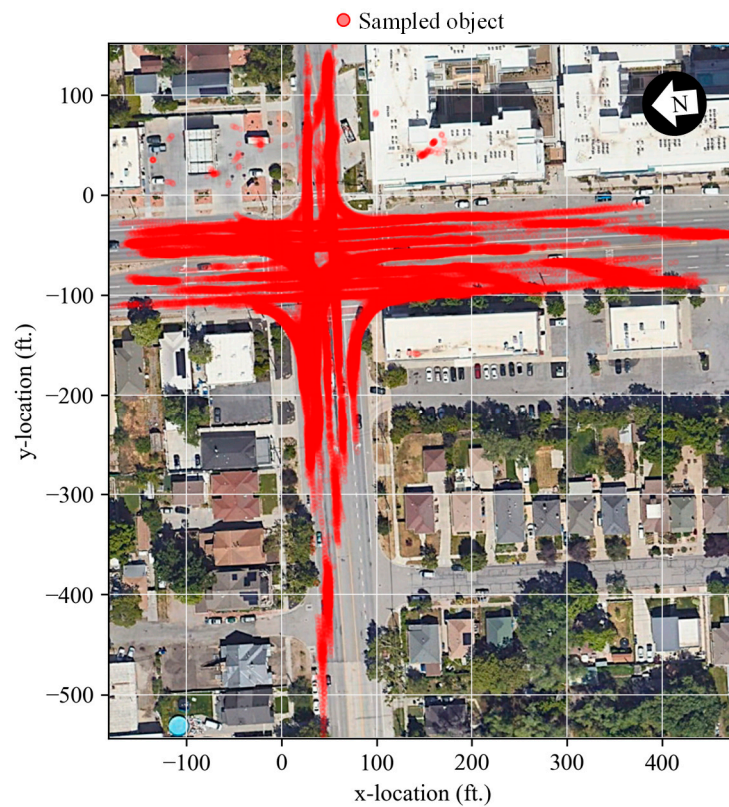
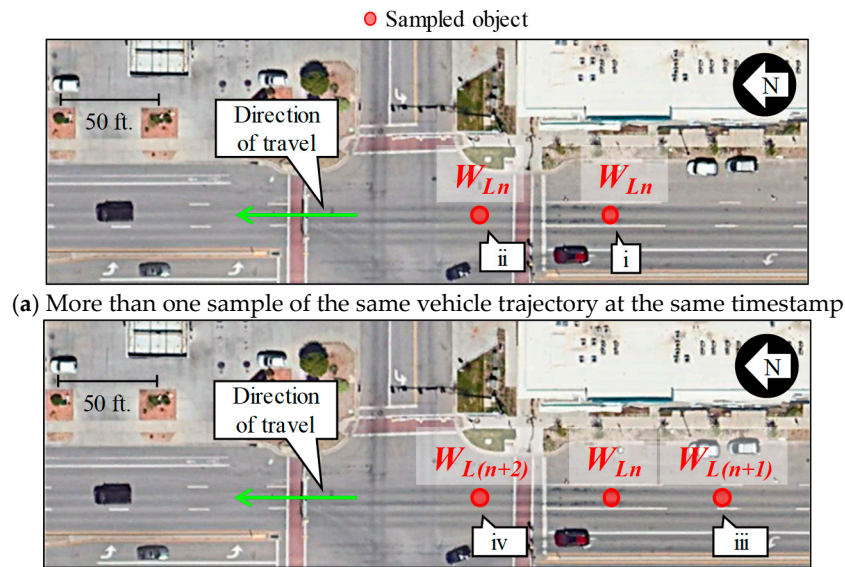


Figure 2. All sampled moving objects detected from the LiDAR sensors (map data: Google) (n: 131,093).

The following subsections discuss each of these steps.

3.2.1. Noise

Two different types of noise were identified, which could significantly affect the accurate estimation of traffic signal performance measures. Figure 3 shows an example of each case.



(b) The location of a sample does not concur with the vehicle trajectory's previous direction of travel

Figure 3. Noise in the LiDAR-derived geospatial dataset (map data: Google).

The first type of noise (Figure 3a) occurs when two waypoints of a trajectory T_L are estimated to occur at the same timestamp n at different locations. Since a vehicle cannot be in two locations at the same time, one waypoint needs to be discarded from T_L . This selection needs to be carefully made as either choice can result in different signal performance estimations being made for the traversing vehicle. For example, in the hypothetical case of a vehicle traveling NB-through presented in Figure 3a, selecting callout i would likely result in a larger estimated delay than if callout ii was selected. This is because callout i is farther away from exiting the intersection at the same timestamp as callout ii.

The second type of noise (Figure 3b) occurs when the waypoint sampled after the current timestamp n (i.e., $n + 1$, callout iii) is located opposite to the vehicle's direction of travel (i.e., the n waypoint's heading). Usually, the subsequent sample after the erroneous case (i.e., $n + 2$, callout iv) is congruously located in relation to the original direction of travel. In these scenarios, the sample that appeared in an unexpected location (in this case $n + 1$) needs to be discarded.

The discussed noise in this subsection could be the result of the sensor configuration, environmental conditions, or the trajectory generation algorithms. Further investigation into these challenges is beyond the scope of this study and additional research should focus on these topics. The following subsection describes how to handle trajectories with noise.

3.2.2. Verification

LiDAR-sampled vehicle trajectories need to be verified, and erroneous samples discarded, based on the challenges discussed in Figure 3. The proposed technique to accomplish this objective chronologically iterates through each waypoint of each trajectory, projects future locations, and keeps subsequent samples that are close enough to the estimated destinations. The step-by-step process used to verify a trajectory's T_L waypoints sampled at contiguous timestamps n and $n + 1$ is provided below and is graphically depicted in Figure 4:

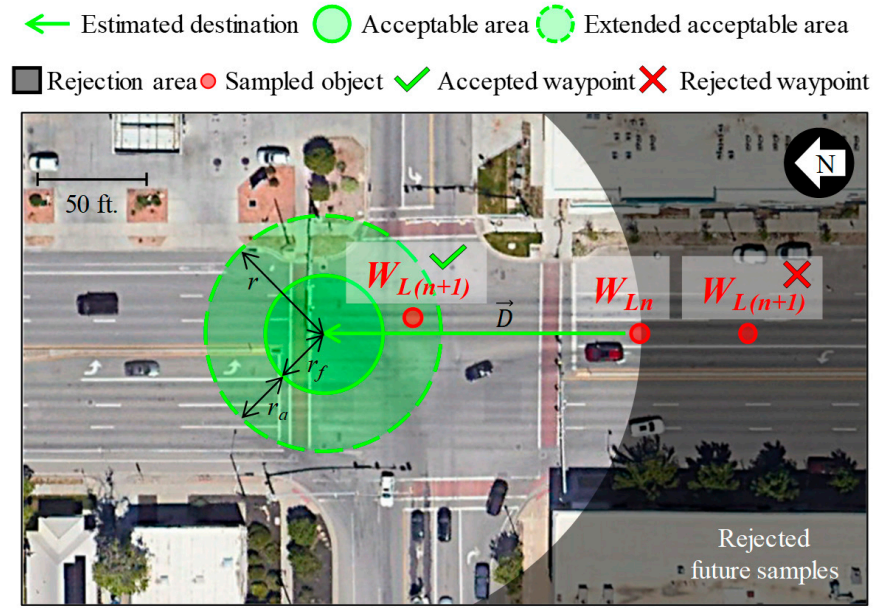


Figure 4. Trajectory segment verification from n to $n + 1$, where $n + 1$ is a timestamp with two sampled waypoints (map data: Google).

1. A destination vector \vec{D} for waypoint W_{Ln} sampled at timestamp (t) n , which points at the expected location of the next waypoint $W_{L(n+1)}$ sampled at $n + 1$, is calculated as follows:

$$\Delta t = t_{n+1} - t_n \tag{5}$$

$$D = \left| \vec{D} \right| = \Delta t \times \text{speed}_n \tag{6}$$

$$\vec{D} = D \cos(\text{heading}_n) \hat{i} + D \sin(\text{heading}_n) \hat{j}, \text{ heading}_n \in [0, 2\pi) \tag{7}$$

where t_n (seconds), speed_n (m/s), and heading_n (radians) are the attributes of W_{Ln} and t_{n+1} is the timestamp of $W_{L(n+1)}$. Heading values increase counterclockwise, where zero points to the positive direction of the x-axis. Unit vectors \hat{i} and \hat{j} denote the positive directions in the x-axis and the y-axis, respectively.

2. From the position indicated by \vec{D} , an acceptable location area for $W_{L(n+1)}$ with radius r (meters), is defined as follows:

$$r = \min(r_f + r_a, D) \tag{8}$$

where r_f (meters) is an arbitrary fixed value (10 m in this study) that always allows for some variation in the sampling results, and r_a (meters) dynamically extends r by considering the likely vehicle acceleration a (m/s^2). The calculation of r_a is as follows:

$$r_a = \frac{1}{2} a (\Delta t)^2 \tag{9}$$

In this study, a equals 3 m/s^2 , which is a probable vehicle acceleration and acceleration at signalized intersections [33,34]. If $r_f + r_a$ is longer than D , then r equals D to avoid accepting samples that go against the direction of travel (Figure 3b).

3. Keep in IT_L the waypoint sampled at $n + 1$ closest to the position indicated by \vec{D} if it lies within the acceptable area with radius r . If that is the case, go back to the first step and repeat the process with the $n + 1$ waypoint as n .

If no waypoint sampled at $n + 1$ is found within the acceptable area, discard them. Then, return to the first step to repeat the process, now comparing the waypoint sampled

at n with the waypoints sampled at $n + 1 + i$, where i is a count of how many iterations have failed to update n .

This process is run for all trajectories and starts with the first sampled waypoint. In most cases, the presented technique successfully filters incorrect waypoints for the noise discussed in Figure 3.

A limitation of this approach is that it assumes that the first sampled waypoint is not noise, as future projections depend on it. However, even if the initially sampled waypoint is not accurate, the acceptable threshold r eventually accepts correct samples. The following subsection describes how to keep only relevant data to analyze the movement-level traffic signal performance.

3.2.3. Selection

After the noise in the raw data (Figure 2) has been identified (Figure 3), and vehicle trajectories have been verified (Figure 4), the pertinent data to evaluate the traffic signal performance for the movement of interest need to be selected.

In this study, the objective was to analyze traffic signal performance for the NB-through movement. To ensure a focused analysis based on trajectories that significantly contribute to the estimation of performance metrics, only the trajectories that comply with all the following predicates were chosen:

- All waypoints have a heading between 150° and 210° , where the heading values increase counterclockwise, with zero pointing to the positive direction of the x -axis;
- The trajectory crosses the movement's far side (callout i);
- The trajectory traveled at least 75 m (~246 ft.).

Figure 5 shows the result of applying these predicates, in addition to the trajectory verification algorithm (Figure 4), to the raw data (Figure 2). Only vehicles that traveled NB-through over a significant distance were selected. This subset of the LiDAR data could then be analyzed to derive movement-level traffic signal performance measures.



Figure 5. Data selection for NB-through movement analysis (n: 7062) (map data: Google).

It is important to note the data gap shown in callout ii. This is likely the result of the dataset not containing the waypoints of vehicles traveling under 10 mph, in combination with the effects that the sensor configuration and environmental conditions have on data sampling. Further investigation is beyond the scope of this study and future research should further investigate this.

3.3. Linear-Referencing LiDAR Data in a PPD

PPDs derived from the selected LiDAR data in Figure 5 can be used to estimate traffic signal performance measures for the NB-through movement at the intersection of US-89 and 600 N (Figure 1). A PPD is a time–space diagram that shows the experience of traversing trajectories at an intersection. Figure 6 shows how a verified vehicle trajectory identified as traveling NB-through is linear-referenced to create a PPD from its geospatial representation.

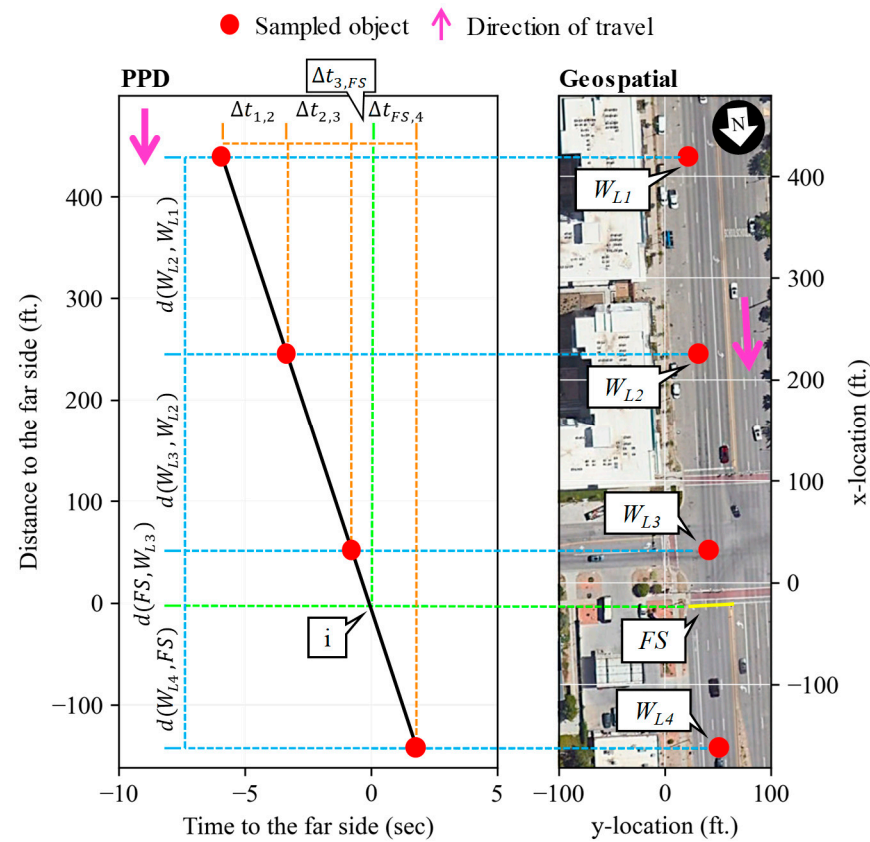


Figure 6. Linear referencing of a vehicle trajectory in a PPD (FS: far side) (map data: Google).

In a PPD, plotted trajectories pivot on the far side of the intersection (Figure 6, callout FS), which means that the time and space at which the vehicle is estimated to cross over this line is taken as the origin (Figure 6, callout i). The vertical axis represents the distance (ft.) from a sampled waypoint to the far side, where $d(A, B)$ is the distance between points A and B. The horizontal axis represents the time needed (s) for a vehicle trajectory to reach the far side, where $\Delta t_{B,A}$ is the time difference between points B and A.

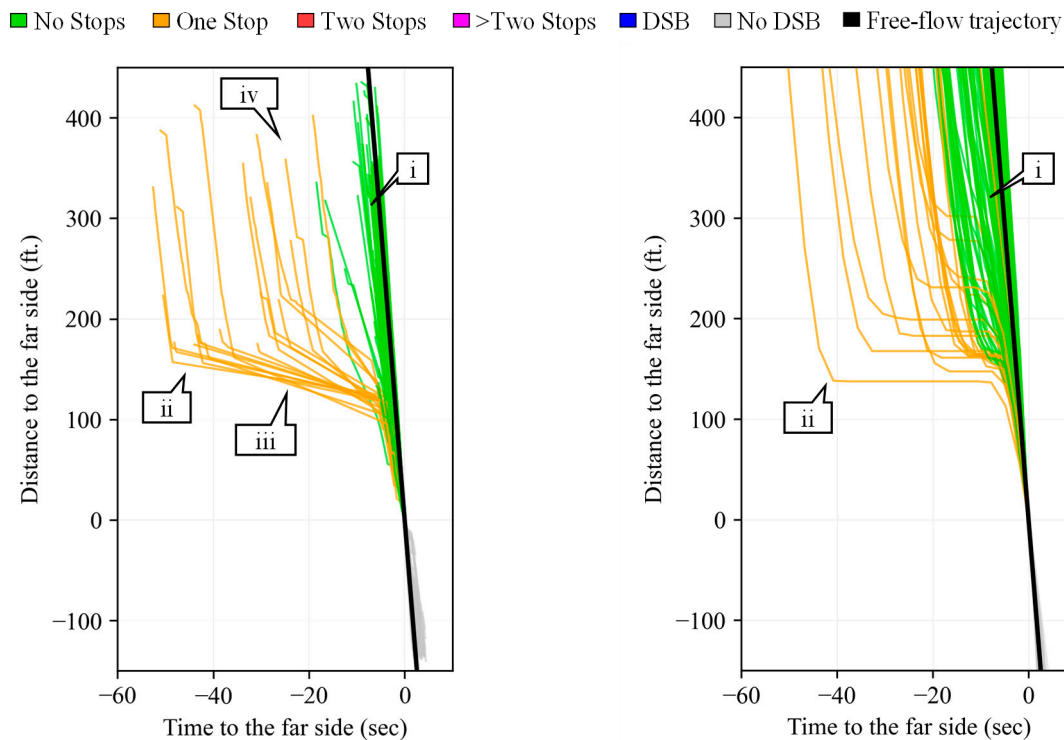
Based on how long it took a vehicle to cross through the intersection, and how many times and where it stopped, AOG, SF, DSB, and control delay can be calculated. A detailed PPD explanation, how to construct them from verified vehicle trajectories, and how to derive performance measures from this are available in the open access Next Generation Traffic Signal Performance Measures: Leveraging Connected Vehicle Data report [23].

4. Comparison of PPDs Generated by LiDAR and CV Data

This section presents and compares PPD operational and delay performance estimations derived from LiDAR data collected from 15:49:25 to 17:14:00 h on 30 December 2022, and from CV trajectory data collected on weekdays in August 2021 during the same time frame. The temporal differences between the analyzed datasets are a result of their limited availability. Nevertheless, since AADT in 2022 (LiDAR data availability) is only 2% higher than in 2021 (CV data availability), a performance comparison between the two is valid [32]. To generate comparable PPDs from both datasets in terms of the amount of data analyzed, the CV trajectory data analysis period is 22 times larger than that for LiDAR due to its low currently commercial MPR.

4.1. Operations-Oriented Purdue Probe Diagram

Figure 7 shows a LiDAR-derived (Figure 7a) and a CV-derived (Figure 7b) PPD, color-coded based on the estimated number of stops that each sampled vehicle experienced during its approach. Overall, the shape of the PPDs is similar. Both present a significant proportion of vehicles that do not have to stop before crossing through the intersection (green, callout i). Furthermore, the maximum amount of time that stopping vehicles (orange) have to wait before continuing their progression is alike (callout ii). Nevertheless, some important differences do exist.



(a) LiDAR-derived (30 December 2022, from 15:49:25 to 17:14:00 h) (n: 189) (b) CV-derived (August 2021 weekdays from 15:49:25 to 17:14:00 h) (n: 218)

Figure 7. Color-coded PPDs by number of stops.

The one-stop trajectories in Figure 7a show a particular shape, where instead of presenting horizontal segments during the time that vehicles are stopped, diagonal segments are shown (callout iii). This occurs because the LiDAR dataset does not include any way-point of vehicles traveling under 10 mph. Therefore, for each vehicle that stops, there is a data gap between when it slows down and when it speeds up over the 10 mph threshold. Due to this limitation, this study assumes that a vehicle trajectory stops if there is a data gap

longer than 5 s between two consecutive waypoints where the necessary speed to travel between them is less than 5 mph.

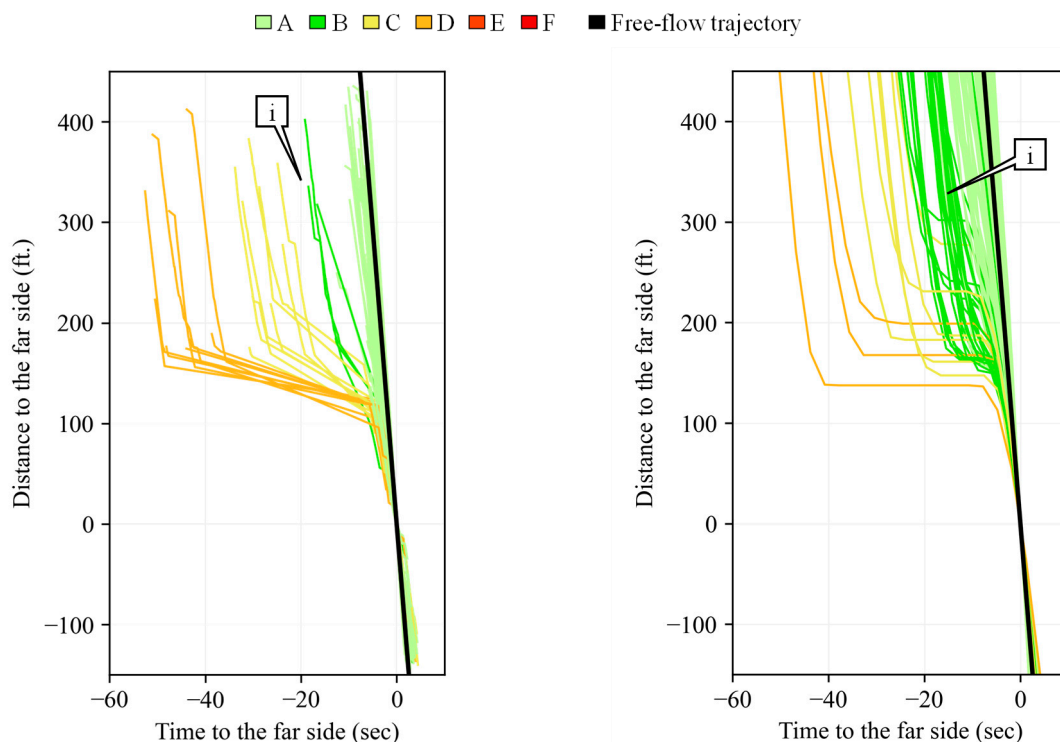
Additionally, LiDAR-sampled vehicle trajectories are not visible much farther than 400 ft. upstream of the far side (callout iv) due to sensor limitations. In contrast, the CV dataset provides trajectory locations from the time vehicles are turned on until they are turned off. Table 2 provides a comparison of AOG, SF, and DSB estimations from each source [23]. Similar results are shown. The only difference is that AOG decreased 1% during the period analyzed with LiDAR data, likely due to the different data sources’ intricacies and the 2% increase in AADT from 2021 to 2022.

Table 2. Operational performance measures by source.

Measurement	LiDAR	CV	Difference
AOG	89%	90%	−1%
SF	0%	0%	0%
DSB	0%	0%	0%

4.2. Delay-Oriented Purdue Probe Diagram

Figure 8 shows the same PPDs as Figure 7, but the trajectories are color-coded based on their estimated control delay LOS (Table 1). Table 3 provides a data source comparison of delay-focused performance estimations. Both PPDs are assigned an LOS A, and only an increase of 1.39 sec/veh in the weighted average control delay is estimated from the LiDAR data. This change is consistent with the 2% AADT increase that occurred during the LiDAR analysis period. The largest discrepancy is the percentage of vehicles assigned an LOS B (callout i).



(a) LiDAR-derived (30 December 2022, from 15:49:25 to 17:14:00 h) (n: 189) (b) CV-derived (August 2021 weekdays from 15:49:25 to 17:14:00 h) (n: 218)

Figure 8. Color-coded PPDs by LOS.

Table 3. Delay performance measures by source.

Measurement	LiDAR	CV	Difference
Avg. control delay (s/veh)	4.51	3.12	+1.39
Movement LOS	A	A	
Sampled vehicles with LOS A	88%	83%	+5%
Sampled vehicles with LOS B	2%	12%	−10%
Sampled vehicles with LOS C	5%	3%	+2%
Sampled vehicles with LOS D	5%	1%	+4%
Sampled vehicles with LOS E	0%	0%	0%
Sampled vehicles with LOS F	0%	0%	0%

5. Discussion

Both evaluated data sources obtained similar performance measures for vehicles following the same movement at the same signalized intersection. The only discrepancies (Tables 2 and 3) are 1% in AOG, a 1.39 s/veh in average control delay, and $\leq 10\%$ in the distribution of LOS. These small differences indicate that the proposed techniques can generate accurate LiDAR-derived movement-level traffic signal performance estimations. The minor discrepancies in the results are likely a consequence of the analyses being based on different time periods that differ by 2% in AADTs. Additionally, the different intricacies of each analyzed data source, such as data collection rates, MPR, and detection areas, also affect traffic signal performance estimations.

An advantage of using LiDAR-derived vehicle trajectories for performance estimations is that virtually all traversing vehicles are represented; therefore, shorter time frames are required for analysis than those needed in studies that use CV data. Additionally, based on LiDAR's mode detection and tracking capabilities, it is possible to extend existing and create new traffic signal performance measures that include various modes of transportation.

The main challenge in deriving traffic signal performance from LiDAR trajectories is that upstream vehicle detection may be limited. In this study, only a few vehicle trajectories were detected past 400 ft. upstream from the far side (Figure 7a, callout iv). However, at intersections with longer queues, missing vehicles stopping far upstream can lead to inaccurate performance estimations. For example, Figure 9 shows the CV-based PPD of a movement at a signalized intersection where the first stops of many split failing vehicles occur upstream of the 400 ft. mark (callout i). Most of these events would have likely been missed by the LiDAR system analyzed in this study, which would result in underestimated delay, SF, and overestimated AOG.

If agencies intend to estimate traffic signal performance using LiDAR, the authors recommend implementing a configuration and number of sensors that would provide detection that can cover the largest observed queues at the intersection. The authors also recommend not to filter dataset waypoints by means of traveling speeds, or any other attribute, to reduce the data footprint. Counting with the entire dataset can provide a more complete picture of the operational condition at traffic signals.

Future research should focus on performing a similar comparison at a location with congestion challenges where split failure and downstream blockage events occur. This is because the current analysis does not exhibit any indication that these events happen at the studied location; therefore, an evaluation of the accuracy of SF and DSB estimations is not possible at the studied intersection. However, based on the generated PPDs, it is expected that the presented technique can also provide reliable SF and DSB estimations. Furthermore, a comparison of the traffic signal performance estimations derived from state-of-the-practice detector-based Automated Traffic Signal Performance Measures (ATSPM) [20] and LiDAR sensors should be performed to further validate the results of the latter.

It is worth noting that the challenges associated with generating the LiDAR-based performance metrics discussed in this study, in particular the data noise (Figure 3) and geospatial detection limitations (Figure 7a, callout iv), are inherent to the LiDAR system

deployed at the US-89 and 600 N intersection during the data collection period. These challenges may or may not arise on other installed LiDAR systems.

■ No Stops ■ One Stop ■ Two Stops ■ >Two Stops ■ DSB ■ No DSB ■ Free-flow trajectory

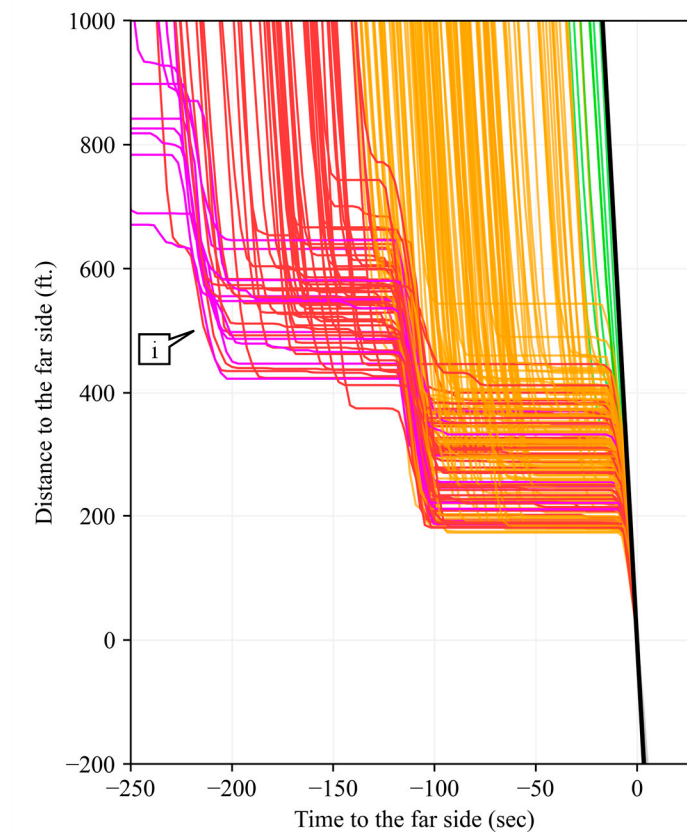


Figure 9. Split failures identified far upstream with CV data.

6. Conclusions

This study provided a technique to generate PPDs from LiDAR-derived data to allow for the estimation of trajectory-based traffic signal performance measures. To demonstrate the methodology, over one hour of LiDAR data collected at a signalized intersection in Utah were used to calculate movement-level AOG, SF, DSB, and control delay LOS. The results were compared to those obtained from a baseline technique that uses high-fidelity CV data. The main contributions of this study are as follows:

- Two types of possible data noise that can negatively affect the creation of LiDAR-based PPDs were identified (Figure 3) and an approach to filter such samples is provided (Figure 4).
- The proposed technique can successfully estimate movement-level traffic signal performance measures. Only 1% AOG and 1.39 s/veh weighted average control delay differences were observed with the baseline approach (Figures 7 and 8).

Practitioners can expand the capabilities of their LiDAR deployments by estimating traffic signal performance measures with the presented methodology. It is recommended to not reduce LiDAR datasets to decrease the data footprint with the objective of providing as much detail as possible on the operational conditions of the analyzed intersections. Furthermore, it is important to note that in order to accurately estimate traffic signal performance from LiDAR systems, sensor quantity and configuration needs to provide vehicle detection up to the largest queues observed at the studied locations.

Author Contributions: Conceptualization, E.D.S.-C. and D.M.B.; methodology, E.D.S.-C.; software, E.D.S.-C.; validation, E.D.S.-C.; formal analysis, E.D.S.-C.; investigation, E.D.S.-C.; resources, D.M.B.; data curation, E.D.S.-C.; writing—original draft preparation, E.D.S.-C.; writing—review and editing, D.M.B.; visualization, E.D.S.-C.; supervision, D.M.B.; project administration, D.M.B.; funding acquisition, D.M.B. All authors have read and agreed to the published version of the manuscript.

Funding: This work was supported in part by the Joint Transportation Research Program and Pooled Fund Study (TPF-5(519)) led by the Indiana Department of Transportation (INDOT) and supported by the state transportation agencies of California, Connecticut, Georgia, Minnesota, Mississippi, North Carolina, Ohio, Pennsylvania, Texas, and Utah, and the Federal Highway Administration (FHWA) Operations Technical Services Team. The contents of this paper reflect the views of the authors, who are responsible for the facts and the accuracy of the data presented herein, and do not necessarily reflect the official views or policies of the sponsoring organizations. These contents do not constitute a standard, specification, or regulation.

Institutional Review Board Statement: Not applicable.

Informed Consent Statement: Not applicable.

Data Availability Statement: The original LiDAR data presented in the study are openly available in <https://www.doi.org/10.4231/MYZ4-8S55> (accessed on 2 April 2024). The aggregated CV datasets generated and/or analyzed during the study are available from the corresponding author on reasonable request.

Acknowledgments: August 2021 weekday connected vehicle trajectory data used in this study was provided by Wejo Data Services, Inc.

Conflicts of Interest: The authors declare no conflicts of interest.

References

- Roriz, R.; Cabral, J.; Gomes, T. Automotive LiDAR Technology: A Survey. *IEEE Trans. Intell. Transp. Syst.* **2022**, *23*, 6282–6297. [CrossRef]
- Chang, J.C.; Findley, D.J.; Cunningham, C.M.; Tsai, M.K. Considerations for Effective Lidar Deployment by Transportation Agencies. *Transp. Res. Rec. J. Transp. Res. Board.* **2014**, *2440*, 1–8. [CrossRef]
- Raj, T.; Hashim, F.H.; Huddin, A.B.; Ibrahim, M.F.; Hussain, A. A Survey on LiDAR Scanning Mechanisms. *Electronics* **2020**, *9*, 741. [CrossRef]
- Liu, W.; Chen, S.; Hauser, E. Lidar-Based bridge structure defect detection. *Exp. Tech.* **2011**, *35*, 27–34. [CrossRef]
- Zhao, J.; He, X.; Li, J.; Feng, T.; Ye, C.; Xiong, L. Automatic Vector-Based Road Structure Mapping Using Multibeam LiDAR. *Remote Sens.* **2019**, *11*, 1726. [CrossRef]
- Li, Z.; Cheng, C.; Kwan, M.-P.; Tong, X.; Tian, S. Identifying Asphalt Pavement Distress Using UAV LiDAR Point Cloud Data and Random Forest Classification. *ISPRS Int. J. Geoinf.* **2019**, *8*, 39. [CrossRef]
- De Blasiis, M.R.; Di Benedetto, A.; Fiani, M.; Garozzo, M. Assessing of the Road Pavement Roughness by Means of LiDAR Technology. *Coatings* **2020**, *11*, 17. [CrossRef]
- Gargoum, S.; El-Basyouny, K.; Sabbagh, J.; Froese, K. Automated Highway Sign Extraction Using Lidar Data. *Transp. Res. Rec. J. Transp. Res. Board.* **2017**, *2643*, 1–8. [CrossRef]
- Guan, H.; Yan, W.; Yu, Y.; Zhong, L.; Li, D. Robust Traffic-Sign Detection and Classification Using Mobile LiDAR Data with Digital Images. *IEEE J. Sel. Top. Appl. Earth Obs. Remote Sens.* **2018**, *11*, 1715–1724. [CrossRef]
- Zhao, J.; Xu, H.; Liu, H.; Wu, J.; Zheng, Y.; Wu, D. Detection and tracking of pedestrians and vehicles using roadside LiDAR sensors. *Transp. Res. Part. C Emerg. Technol.* **2019**, *100*, 68–87. [CrossRef]
- Kidono, K.; Miyasaka, T.; Watanabe, A.; Naito, T.; Miura, J. Pedestrian recognition using high-definition LIDAR. In *2011 IEEE Intelligent Vehicles Symposium (IV)*; IEEE: Baden-Baden, Germany, 2011; pp. 405–410. [CrossRef]
- Bandaru, V.K.; Romero, M.A.; Lizarazo, C.; Tarko, A.P. *TScan—Stationary LiDAR for Traffic and Safety Applications: Vehicle Interpretation and Tracking*; Purdue University: West Lafayette, IN, USA, 2022. [CrossRef]
- Ansariyar, A. Providing a Comprehensive Traffic Safety Analysis Collected by Two LiDAR Sensors at a Signalized Intersection. *Preprints* **2023**, *2023*, 2023101401. [CrossRef]
- Kilani, O.; Gouda, M.; Weiß, J.; El-Basyouny, K. Safety Assessment of Urban Intersection Sight Distance Using Mobile LiDAR Data. *Sustainability* **2021**, *13*, 9259. [CrossRef]
- ITE and NOCoE. 2019 Traffic Signal Benchmarking and State of the Practice Report. 2020. Available online: <https://transportationops.org/trafficsignals/benchmarkingreport> (accessed on 1 April 2024).
- National Transportation Operations Coalition. National Traffic Signal Report Card, Washington DC, 2012. Available online: https://transops.s3.amazonaws.com/uploaded_files/NTOC-2012-Traffic-Signal-Report-Card-Technical-Report.pdf (accessed on 1 April 2024).

17. Sunkari, S. The Benefits of Retiming Traffic Signals. *Inst. Transp. Eng. ITE J.* **2004**, *74*, 26–29.
18. Denney, R.W.; Head, L.; Spencer, K. *Signal Timing Under Saturated Conditions*; United States. Federal Highway Administration: Washington, DC, USA, 2008.
19. Gayen, S. *Statewide Identification and Ranking of Signalized Intersections Needing Capacity Improvements*; Purdue University: West Lafayette, IN, USA, 2024.
20. Day, C.M.; Bullock, D.M.; Li, H.; Remias, S.M.; Hainen, A.M.; Freije, R.S.; Stevens, A.L.; Sturdevant, J.R.; Brennan, T.M. *Performance Measures for Traffic Signal Systems: An Outcome-Oriented Approach*; Purdue University: West Lafayette, IN, USA, 2014. [[CrossRef](#)]
21. Saldivar-Carranza, E.; Li, H.; Gayen, S.; Taylor, M.; Sturdevant, J.; Bullock, D. Comparison of Arrivals on Green Estimations from Vehicle Detection and Connected Vehicle Data. *Transp. Res. Rec. J. Transp. Res. Board* **2023**, *2677*, 328–342. [[CrossRef](#)]
22. Saldivar-Carranza, E.D.; Gayen, S.; Li, H.; Bullock, D.M. Comparison at Scale of Traffic Signal Cycle Split Failure Identification from High-Resolution Controller and Connected Vehicle Trajectory Data. *Future Transp.* **2024**, *4*, 236–256. [[CrossRef](#)]
23. Saldivar-Carranza, E.D.; Li, H.; Mathew, J.K.; Desai, J.; Platte, T.; Gayen, S.; Sturdevant, J.; Taylor, M.; Fisher, C.; Bullock, D.M. *Next Generation Traffic Signal Performance Measures: Leveraging Connected Vehicle Data*; Purdue University: West Lafayette, IN, USA, 2023. [[CrossRef](#)]
24. Waddell, J.M.; Remias, S.M.; Kirsch, J.N. Characterizing Traffic-Signal Performance and Corridor Reliability Using Crowd-Sourced Probe Vehicle Trajectories. *J. Transp. Eng. A Syst.* **2020**, *146*, 04020053. [[CrossRef](#)]
25. Waddell, J.M.; Remias, S.M.; Kirsch, J.N.; Young, S.E. Scalable and Actionable Performance Measures for Traffic Signal Systems using Probe Vehicle Trajectory Data. *Transp. Res. Rec. J. Transp. Res. Board* **2020**, *2674*, 304–316. [[CrossRef](#)]
26. Mahmud, S.; Day, C.M. Evaluation of Arterial Signal Coordination with Commercial Connected Vehicle Data: Empirical Traffic Flow Visualization and Performance Measurement. *J. Transp. Technol.* **2023**, *13*, 327–352. [[CrossRef](#)]
27. Transportation Research Board. *Highway Capacity Manual 2010*; National Research Council (NRC): Washington, DC, USA, 2010.
28. Sakhare, R.S.; Hunter, M.; Mukai, J.; Li, H.; Bullock, D.M. Truck and Passenger Car Connected Vehicle Penetration on Indiana Roadways. *J. Transp. Technol.* **2022**, *12*, 578–599. [[CrossRef](#)]
29. Ansariyar, A. Precision in Motion: Assessing the Accuracy of LiDAR Sensors for Delay Time Calculation at Signalized Intersections. *SSRN* **2023**, *2023*, 4595005. [[CrossRef](#)]
30. Li, T.; Taylor, M.; Saldivar-Carranza, E.D.; Bullock, D.M. Traffic Signal LiDAR-derived Vehicle Trajectories Dataset. In *Purdue University Research Repository*; Purdue University: West Lafayette, IN, USA, 2024. [[CrossRef](#)]
31. Li, Y.; Ibanez-Guzman, J. Lidar for Autonomous Driving: The Principles, Challenges, and Trends for Automotive Lidar and Perception Systems. *IEEE Signal Process. Mag* **2020**, *37*, 50–61. [[CrossRef](#)]
32. Utah Department of Transportation. AADT GOOGLE MAP. Available online: <https://www.udot.utah.gov/connect/docs/aadt-google-map/> (accessed on 10 April 2024).
33. Long, G. Acceleration Characteristics of Starting Vehicles. *Transp. Res. Rec.* **2000**, *1737*, 58–70. [[CrossRef](#)]
34. El-Shawarby, I.; Rakha, H.; Inman, V.W.; Davis, G.W. Evaluation of Driver Deceleration Behavior at Signalized Intersections. *Transp. Res. Rec. J. Transp. Res. Board.* **2018**, *1*, 29–35. [[CrossRef](#)]

Disclaimer/Publisher’s Note: The statements, opinions and data contained in all publications are solely those of the individual author(s) and contributor(s) and not of MDPI and/or the editor(s). MDPI and/or the editor(s) disclaim responsibility for any injury to people or property resulting from any ideas, methods, instructions or products referred to in the content.